BIOORGANIC CHEMISTRY **24,** 340–357 (1996)
ARTICLE NO. 0030

Influence of L-Cysteine on the Oxidation Chemistry of (-)-Epinephrine: Formation of Cysteinyl Conjugates and Novel Dihydrobenzothiazines

XUE-MING SHEN AND GLENN DRYHURST[1]

Department of Chemistry and Biochemistry, University of Oklahoma, Norman, Oklahoma 73019

Received June 5, 1996

Oxidation of epinephrine (EPI) in aqueous solution at pH 7.4 generates an *ortho*-quinone **(1)** that normally deprotonates and undergoes a rapid intramolecular cyclization and secondary reactions, ultimately leading to an indolic melanin polymer. In this investigation, it is demonstrated that L-cysteine (CySH) can intervene in this reaction by scavenging *o*-quinone **1** to give 5-*S*-cysteinylepinephrine (5-*S*-CyS-EPI) and 2-*S*-cysteinylepinephrine (2-*S*-CyS-EPI). Subsequent oxidation ($2e$, $2H^+$) of the latter cysteinyl conjugates gives *o*-quinones that can either react further with free CySH to give the 2,5-bi-*S*- and 2,5,6-tri-*S*-cysteinyl conjugates of EPI or cyclize to give 7-[(2-methylamino)ethyl]-3,4-dihydro-5-hydroxy-2*H*-1,4-benzothiazine-3-carboxylic acid (DHBT-E1) and 8-[(2-methylamino)ethyl]-3,4-dihydro-5-hydroxy-2*H*-1,4-benzothiazine-3-carboxylic acid (DHBT-E2), respectively, Oxidations of 2,5-bi-*S*-CyS-EPI and 2,5,6-tris-*S*-CyS-EPI and of DHBT-E1 and DHBT-E2 in the presence of CySH provide routes to a number of other dihydrobenzothiazines (DHBTs). Four new cysteinyl conjugates of EPI and seven DHBTs have been isolated and their structures elucidated by spectroscopic methods. Based upon a number of lines of converging evidence, it is suggested that these compounds might include unusual metabolites of EPI formed in adrenergic neurons under certain pathological brain conditions.

INTRODUCTION

Recently, it was proposed (*1*, *2*) that a very early event in the pathogenesis of idiopathic Parkinson's Disease (PD) is the upregulation of γ-glutamyl transpeptidase (γ-GT) (*3*) with consequent translocation of L-cysteine (CySH) (*4*, *5*), biosynthesized and exported by glial cells (*6*, *7*), into neuromelanin-pigmented dopaminergic cell bodies in the substantia nigra (SN). These cell bodies are normally pigmented because of autoxidation of cytoplasmic dopamine (DA) to DA-*o*-quinone that subsequently undergoes intramolecular cyclization and oxidative polymerization to black neuromelanin (*8–11*). Based upon *in vitro* studies (*1*, *2*, *12*), such a γ-GT-mediated translocation of CySH into pigmented SN cells that, in common with other neuronal cell bodies, normally contain little or no CySH or glutathione (GSH) (*13*), would be expected to divert the neuromelanin pathway by scavenging DA-*o*-quinone to give initially 5-*S*-cysteinyldopamine (5-*S*-CyS-DA) and 2-*S*-cysteinyl-

[1] To whom correspondence should be addressed. Fax: (405)-325-6111. E-mail: gdryhurst@chemdept.chem.uoknor.edu.

0045-2068/96 $18.00

dopamine (2-*S*-CyS-DA). These cysteinyl conjugates are more easily oxidized than DA (*1*, *2*) to give more complex cysteinyldopamines and a number of dihydrobenzothiazines (DHBTs). Several of these putative intraneuronal metabolites are lethal when administered into the brains of mice and rats and evoke a very characteristic neurobehavioral response (hyperactivity and tremor) (*1*, *2*). These observations have led to the suggestion that such compounds might include the endotoxin(s) responsible for the degeneration of nigrostriatal dopaminergic neurons, one pathological hallmark of PD (*14*). Noradrenergic neurons projecting from the neuromelanin-pigmented locus ceruleus (LC) also degenerate in PD (*15*, *16*). Neuromelanin pigment in noradrenergic LC cells bodies results from autoxidation of norepinephrine (NE) to NE-*o*-quinone that polymerizes by a similar pathway to DA-*o*-quinone (*8*). Thus, it has been proposed that an upregulation of γ-GT and translocation of CySH into pigmented LC cells might also result in the intraneuronal formation of cysteinyl conjugates of NE and subsequent oxidation to lethal DHBTs that include endotoxins responsible for the degeneration of these neurons in PD (*17*). Noradrenergic neurons that project from the LC to the cortex and hippocampus also degenerate in Alzheimer's Disease (AD) (*18*) and as a result of transient cerebral ischemia (*19*). However, unlike PD, in which the neuropathological processes occur in SN and LC cell bodies (*20*, *21*), the neuropathological processes that take place in the brain in AD and following cerebral ischemia are probably initiated in the terminals of noradrenergic and other vulnerable neurons (*22–24*). Nerve terminals differ from cell bodies in that they normally contain significant concentrations of GSH and, presumably, its biosynthetic precursor CySH (*13*). Furthermore, many lines of evidence indicate that terminal regions of the brain vulnerable to degeneration in AD and following an ischemic insult are subject to oxidative stress (*25–31*). Oxidative stress, i.e., damage deriving from reduced oxygen species ($HO^{\cdot}$, $O_2^{\cdot-}$, H_2O_2), is widely believed to primarily affect membrane lipids, proteins, and nucleic acids (*32*). However, from a chemical perspective, it seems unlikely that easily oxidized NE, particularly the unsheltered cytoplasmic pool of this neurotransmitter, could escape oxidation by oxygen radicals or other oxidative systems. Accordingly, we have suggested that in AD and following an ischemic insult, NE is oxidized to NE-*o*-quinone that in nerve terminals is scavenged by endogenous CySH to give the same or similar endotoxins proposed to be formed in LC cell bodies in PD (*17*). Thus, the vulnerability of pigmented catecholaminergic cell bodies to degeneration in PD is hypothesized to be linked to the fact that DA and NE are normally autoxidized to neuromelanin in these neurons. The neuropathological processes in PD are, therefore, proposed to be triggered by upregualtion of γ-GT and leading to elevated translocation of CySH into these cell bodies with diversion of the neuromelanin pathway to give endotoxic metabolites. By contrast, the vulnerability of certain noradrenergic terminals to degeneration in AD and as a result of an ischemic insult might be related to aberrant oxidation of cytoplasmic NE to NE-*o*-quinone that reacts with endogenous CySH to give the same or similar endotoxins.

(-)-Epinephrine (EPI; adrenaline) is the third catecholaminergic neurotransmitter and is employed by adrenergic neurons in both the central and peripheral nervous systems. Central adrenergic neurons project from cell bodies in the brainstem with both ascending and descending pathways. Ascending pathways terminate primarily

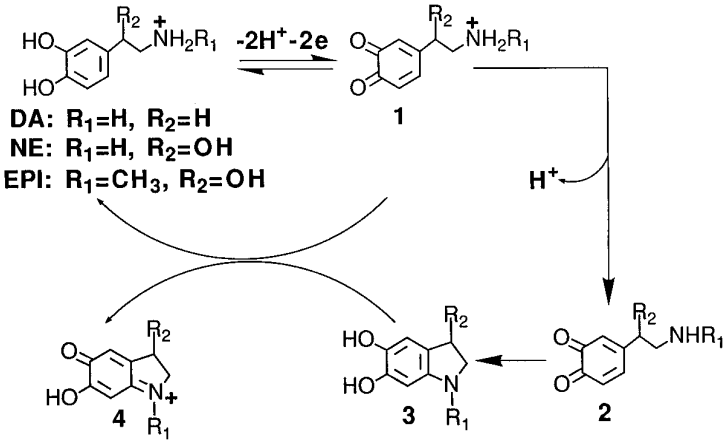

SCHEME 1

in the hypothalamus and, perhaps, more rostrally located structures, whereas descending pathways innervate areas of the spinal cord (*33*). Thus, adrenergic nerve terminals are considerably less widely distributed throughout the brain than are dopaminergic and noradrenergic terminals. Consequently, concentrations of EPI in most regions of the brain are generally much lower than those of DA and NE (*34*). Because of these factors, the heavy overlap between adrenergic and noradrenergic terminal fields, and the similarities between noradrenergic and adrenergic receptors, relatively little is known about the central pharmacology and physiology of adrenergic neurons (*33*). Furthermore, essentially no information is available concerning the degeneration of adrenergic neurons in neurological disorders such as PD and AD. However, as will be demonstrated subsequently, EPI is the most easily oxidized of the catecholaminergic neurotransmitters. Thus, under pathological conditions where DA and NE are oxidized in the brain EPI would also be susceptible to such chemistry. Thus, it is not inconceivable that intraneuronal oxidation of EPI in the presence of CySH might yield aberrant metabolites that play roles in neurodegenerative disorders such as PD and AD similar to those hypothesized to be formed as a result of oxidation of DA and NE. Accordingly, this communication presents the results of the first study into the influence of CySH on the *in vitro* oxidation chemistry of EPI at physiological pH. The principal goals of this investigation were (a) to determine whether CySH diverts the normal oxidation pathway of EPI, and (b) if so, to characterize the major initial products formed. Previous investigators have established that chemical, enzyme-mediated, and electrochemically driven oxidations of DA, NE, and EPI all generate *o*-quinones as the proximate product (*1*, *2*, *8–12*, *35–39*). Electrochemical techniques in particular have permitted further insights into the subsequent reactions of these *o*-quinones, summarized in Scheme 1 (*37*). Thus, deprotonation of the *o*-quinones **(1)** formed upon oxidation ($2e$, $2H^+$) of DA, NE, and EPI yields the neutral *o*-quinones **(2)** that undergo an intramolecular cyclization reaction (1,4-Michael addition) to give 5,6-dihydroxyin-

dolines **(3).** The latter compounds are then oxidized by *o*-quinones **1** to the *para*-quinone imine **4** (often referred to as an aminochrome) (*10*, *11*, *37*). Although the pathways shown in Scheme 1 are fundamentally the same for oxidation of all the catecholaminergic neurotransmitters, the rate of the intramolecular cyclization reaction **(2 → 3)** for the *o*-quinone derived from EPI is much faster than that for the deprotonated *o*-quinones derived from DA and NE (*37*, *40*). Thus, it was of particular interest to ascertain whether nucleophilic addition of CySH to **1**/**2,** formed upon oxidation of EPI, to form cysteinyl conjugates of this neurotransmitter, was sufficiently rapid to compete with intramolecular cyclization of the side chain residue. In accord with recent studies from this laboratory, in this investigation EPI was oxidized to EPI-*o*-quinone using electrochemical methods.

EXPERIMENTAL

Chemicals

(-)-Epinephrine (EPI) and L-cysteine (CySH) were obtained from Sigma (St. Louis, MO). Trifluoroacetic acid (TFA) was obtained from Aldrich (Milwaukee, WI). HPLC grade acetonitrile (MeCN) was obtained from EM Science (Gibbstown, NJ).

Electrochemistry

Voltammograms were obtained at a pyrolytic graphite electrode (PGE; Pfizer Minerals, Pigments and Metals Division, Easton, PA) having an appropriate surface area of 4 mm^2, and were recorded using a BAS-100A (Bioanalytical Systems, West Lafeyette, IN) electrochemical analyzer. A conventional three-electrode cell was employed with a platinum wire counter electrode and a saturated calomel reference electrode (SCE). Controlled potential electrolyses were carried out with a Princeton Applied Research Corporation (Princeton, NJ) Model 173 potentiostat. A three-compartment cell was used in which the working, counter, and reference electrode compartments were separated with a Nafion membrane (type 117, DuPont Co., Wilmington, DE). The working electrode consisted of several plates of pyrolytic graphite (total surface area ca. 180 cm^2) suspended into the working electrode compartment having a solution capacity of 30 ml. The counter electrode was platinum gauze; the reference electrode was a SCE. The solution in the working electrode compartment was vigorously bubbled with N_2 and stirred with a Teflon-coated magnetic stirring bar. All potentials reported are referenced to the SCE at ambient temperature (22 ± 2°C).

Spectroscopy

^{1}H NMR spectra were recorded on a Varian (Palo Alto, CA) XL-300 spectrometer. Low- and high-resolution fast atom bombardment mass spectrometry (FAB-MS) employed a VG Instruments (Manchester, UK) Model ZAB-E spectrometer.

Ultraviolet–visible spectra were recorded on a Hewlett–Packard (Palo Alto, CA) Model 8452A diode array spectrophotometer.

High-Performance Liquid Chromatography (HPLC)

HPLC employed a Gilson (Middleton, WI) gradient system equipped with dual Model 302 pumps (10-ml pump heads), a Rheodyne (Cotati, CA) Model 7125 loop injector, an a Waters (Milford, MA) Model 440 uv detector set at 254 nm. Two mobile-phase solvents were employed. Solvent A was prepared by adding concentrated TFA to deionized water until the pH was 2.15. Solvent B was prepared by adding TFA to 2 liters of MeCN and 2 liters of deionized water until the pH was 2.15. A reversed-phase column (Backerbond C_{18}, 10 μm, 250 $\times$ 21.2 mm, P. J. Cobert Associates, St. Louis, MO) was used with the following mobile phase gradient: 0–85 min, linear gradient from 100% solvent A to 15% solvent B; 85–130 min, linear gradient to 45% solvent B; 130–134 min, linear gradient to 100% solvent B; 134–146 min, 100% solvent B. The flow rate was 7.0 ml min^{-1}.

Oxidation Reaction Procedure, Isolation, Purification, and Structure Elucidation of Products

EPI (2.75 mg; 0.5 mM) and CySH (1.82–18.2 mg; 0.5–5.0 mM) were dissolved in 30 ml of pH 7.4 phosphate buffer (μ = 0.2) and electrolyzed, normally for 30 min at 75 mV. Upon termination of the reaction, the entire yellow solution was pumped into the preparative reversed-phase column and reactants and products were separated by HPLC. The solutions eluted under the chromatographic peaks corresponding to major products were collected separately and immediately frozen at −80°C (dry ice bath). Following several repetitive experiments, the combined solutions containing each product were purified by HPLC and then freeze-dried.

Spectroscopic evidence in support of the proposed structures of products are presented below. The assignments of proton resonances in ^{1}H NMR spectra of products were based on comparisons with the spectra of EPI, CySH, and related compound formed by oxidation of DA and NE in the presence of CySH (*1*, *2*) and in all cases were confirmed by two-dimensional correlated spectroscopy experiments.

5-S-Cysteinylepinephrine (5-S-CyS-EPI)

This compound was isolated as a white solid. In the HPLC mobile phase (pH 2.15), 5-*S*-CyS-EPI exhibited uv bands at λ_{max} 292 and 254 nm. FAB-MS (glycerol/TFA matrix) gave *m/e* = 303.1027 (MH^+, 100%, $C_{12}H_{19}N_2O_5S$; calcd. *m/e* = 303.1015). ^{1}H NMR (D_2O) gave δ 7.04 (d, *J* = 2.1 Hz, 1 H, C(2)-H), 6.91 (d, *J* = 2.1 Hz, 1 H, C(6)-H), 4.89 (dd, *J* = 6.6, 6.0 Hz, 1 H, C(β)-H), 4.05 (dd, *J* = 6.3, 4.8 Hz, 1 H, C(b)-H), 3.44 (dd, *J* = 15.0, 6.3 Hz, 1 H, C(a)-H), 3.36 (dd, *J* = 15.0, 4.8 Hz, 1 H, C(a)-H), 3.22 (m, 2 H, C(α)-H_2), 2.70 (s, 3 H, CH_3).

2-S-Cysteinylepinephrine (2-S-CyS-EPI)

When dissolved in the HPLC mobile phase (pH 2.15) this white solid exhibited uv bands at λ_{max} 292 and 256 nm. FAB-MS (glycerol/TFA matrix) gave *m/e* = 303.1005 (MH^+, 100%, $C_{12}H_{19}N_2O_5S$; cald. *m/e* = 303.1015). ^{1}H NMR (CD_3OD)

gave δ 7.09 (d, J = 8.4 Hz, 1 H, C(5)-H), 6.97 (d, J = 8.4 Hz, 1 H, C(6)-H), 5.56 (dd, J = 9.9, 3.3 Hz, 1 H, C(β)-H), 3.94 (dd, J = 8.7, 4.5 Hz, 1 H, C(b)-H), 3.39 (dd, J = 14.7, 4.5 Hz, 1 H, C(a)-H), 3.25 (dd, J = 14.7, 8.7 Hz, 1 H, C(a)-H), 3.22 (dd, J = 12.6, 3.3 Hz, 1 H, C(α)-H), 3.12 (dd, J = 12.6, 9.9 Hz, 1 H, C(α)-H), 2.79 (s, 3 H, CH_3). ^{1}H NMR (D_2O) gave δ 6.99 (s, 2 H, C(5)-H, C(6)-H) 5.54 (t, J = 6.3 Hz, 1 H, C(β)-H), 4.02 (dd, J = 7.2, 4.8 Hz, 1 H, C(b)-H), 3.36 (dd, J = 15.0, 7.2 Hz, 1 H, C(a)-H), 3.26 (dd, J = 15.0, 4.8 Hz, 1 H, C(a)-H), 3.21 (d, J = 6.3 Hz, 2 H, C(α)-H_2), 2.74 (s, 3 H, CH_3).

2,5-Bi-S-Cysteinylepinephrine (*2,5-Bi-S-CyS-EPI*)

2,5-Bi-*S*-CyS-EPI was a white solid that at pH 2.15 (HPLC mobile phase) exhibited uv bands at λ_{max} 300 (sh) and 272 nm. FAB-MS (3-nitrobenzyl alcohol matrix) gave m/e = 422.1052 (MH^+, 100%, $C_{15}H_{24}N_3O_7S_2$; calcd. m/e = 422.1056). ^{1}H NMR (D_2O) gave δ 7.26 (s, 1 H, C(6)-H), 5.57 (dd, J = 7.5, 4.5 Hz, 1 H, C(β)-H), 4.05 (t, J = 5.1 Hz, 1 H, C(b)-H), 4.03 (t, J = 5.1 Hz, 1 H, C(b′)-H), 3.58 (dd, J = 15.0, 5.1 Hz, 1 H, C(a)-H), 3.57 (dd, J = 15.0, 5.1 Hz, 1 H, C(a′)-H), 3.35 (dd, J = 15.0, 5.1 Hz, 1 H, C(a)-H), 3.22 (dd, J = 15.0, 5.1 Hz, 1 H, C(α)-H), 3.21 (m, 2 H, C(α)-H_2), 2.75 (s, 3 H, CH_3).

2,5,6-Tri-S-Cysteinylephinephrine (*2,5,6-Tri-S-CyS-EPI*)

This compound was a white solid. In the pH 2.15 HPLC mobile phase 2,5,6-tri-*S*-CyS-EPI exhibited uv bands at λ_{max} 312 and 224 nm. FAB-MS (glycerol/TFA/3-nitrobenzyl alcohol matrix) gave m/e = 541.1100 (MH^+, 100%, $C_{18}H_{29}N_4O_9S_3$; calcd. m/e = 541.1097). ^{1}H NMR (D_2O, 50°C) gave δ 6.57 (dd, J = 10.8, 3.6 Hz, 1 H, C(β)-H), 4.38 (t, J = 5.1 Hz, 1 H, 1 H, C(β)″)-H), 4.33 (t, J = 5.4 Hz, 1 H, C(b)-H), 4.31 (t, J = 5.7 Hz, 1 H, C(b′)-H), 4.30 (dd, J = 13.2, 10.8 Hz, 1 H, C(α)-H), 3.95 (dd, J = 15.0, 5.1 Hz, 1 H, C(a″)-H), 3.73–3.64 (m, 4 H, C(a)-H_2, C(a′)-H_2), 3.62 (dd, J = 15.0, 5.1 Hz, 1 H, C(a″)-H), 3.49 (dd, J = 13.2, 3.6 Hz, 1 H, C(α)-H), 3.10 (s, 3 H, CH_3).

7-[(2-Methylamino)ethyl]-3,4-dihydro-5-hydroxy-2H-1,4-Benzothiazine-3-Carboxylic Acid (*DHBT-E1*)

DHBT-E1 was a very pale yellow solid that, when dissolved in the HPLC mobile phase (pH 2.15), exhibited a uv spectrum with λ_{max} 302 and 234 nm. FAB-MS (glycerol/TFA matrix) gave m/e = 285.0916 (MH^+, 57%, $C_{12}H_{17}N_2O_4S$; calcd. m/e = 285.0909). ^{1}H NMR (Me_2SO-d_6) gave δ 12.66 (bs, 1 H, CO_2H), 9.72 (bs, 1 H, C(5)-OH), 8.57 (m, 1 H, NH^+), 8.47 (m, 1 H, NH^+), 6.53 (d, J = 1.8 Hz, 1 H, C(6)-H), 6.41 (d, J = 1.8 Hz, 1 H, C(8)-H), 5.92 (bs, 1 H, C(β)-OH), 5.33 (bs, 1 H, N(4)-H), 4.60 (dd, J = 9.9, 3.0 Hz, 1 H, C(β)-H), 4.35 (dd, J = 5.4, 3.3 Hz, 1 H, C(3)-H), 3.15 (dd, J = 12.6, 3.3 Hz, 1 H, C(2)-H), 3.07 (dd, J = 12.6, 5.4 Hz, 1 H, C(2)-H), 3.02–2.86 (m, 2 H, C(α)-H_2), 2.57 (t, J = 4.2 Hz, 3 H, CH_3). Addition of D_2O caused the resonances at δ 12.66, 9.72, 8.57, 8.47, 5.92, and 5.33 ppm to disappear.

8-[(2-Methylamino)ethyl]-3,4,-dihydro-5-hydroxy-2H-1,4-Benzothiazine-3-Carboxylic Acid (DHBT-E2)

DHBT-E2 was a very pale yellow solid. In the HPLC mobile phase (pH 2.15) it exhibited a uv spectrum at λ_{max} 304 and 228 nm. FAB-MS (3-nitrobenzyl alcohol matrix) gave m/e = 285.0918 (MH^+, 12%, $C_{12}H_{17}N_2O_4S$; calcd. m/e = 285.0909). ^1H NMR (Me_2 SO-d_6) gave δ 12.90 (bs, 1 H, CO_2H), 9.67 (bs, 1 H, C(5)-OH), 8.65 (m, 1 H, NH^+), 8.48 (m, 1 H, NH^+), 6.62 (d, J = 8.1 Hz, 1 H, C(6)-H), 6.57 (d, J = 8.1 Hz, 1 H, C(7)-H), 5.99 (bs, 1 H, C(β)-OH), 5.45 (bs, 1 H, N(4)-H), 4.94 (t, J = 6.6 Hz, 1 H, C(β)-H), 4.41 (dd, J = 5.1, 3.6 Hz, 1 H, C(3)-H), 3.14 (dd, J = 12.6, 5.1 Hz, 1 H, C(2)-H), 3.06 (dd, J = 12.6, 3.6 Hz, 1 H, C(2)-H), 2.90 (dd, J = 12.6, 6.6 Hz, 2 H, C(α)-H_2), 2.59 (t, J = 5.1 Hz, 3 H, CH_3). Addition of D_2O caused the resonances at δ 12.90, 9.67, 8.65, 8.48, 5.99, and 5.45 ppm to disappear.

6-S-Cysteinyl-7[(2-methylamino)ethyl]-3,4-dihydro-5-hydroxy-2H-1,4-Benzothiazine-3-Carboxylic Acid (DHBT-E3)

DHBT-E3 was a very pale yellow solid. When dissolved in the HPLC mobile phase (pH 2.15), DHBT-E3 exhibited a uv spectrum with bands at λ_{max} 318, 280 (sh), and 248 nm. FAB-MS (glycerol/TFA/3-nitrobenzyl alcohol matrix) gave m/e = 404.0928 (MH^+, 40%, $C_{15}H_{22}N_3O_6S_2$; calcd. m/e = 404.0950). ^1H NMR (D_2O) gave δ 6.87 (s, 1 H, C(8)-H), 5.45 (t, J = 6.3 Hz, 1 H, C(β)-H), 4.61 (t, J = 3.9 Hz, 1 H, C(3)-H), 3.89 (t, J = 5.4 Hz, 1 H, C(b)-H), 3.33 (dd, J = 13.2, 3.9 Hz, 1 H, C(2)-H), 3.22 (dd, J = 13.2, 3.9 Hz, 1 H, C(2)-H), 3.21 (m, 2 H, C(α)-H_2), 3.19 (m, 2 H, C(a)-H_2), 2.74 (s, 3 H, CH_3).

6-S-Cysteinyl-8-[(2-methylamino)ethyl]-3,4-dihydro-5-hydroxy-2H-1,4-Benzothiazine-3-Carboxylic Acid (DHBT-E4)

DHBT-E4 was a very pale yellow solid, λ_{max} (pH 2.15 mobile phase) 316, 278 (sh), and 244 nm. FAB-MS (3-nitrobenzyl alcohol matrix) gave 404.0952 (MH^+, 100%, $C_{15}H_{22}N_3O_6S_2$; calcd. m/e = 404.0950). ^1H NMR (D_2O) gave δ 7.02 (s, 1 H, C(7)-H), 5.17 (dd, J = 6.6, 5.1 Hz, 1 H, C(β)-H), 4.65 (t, J = 3.9 Hz, 1 H, C(3)-H), 4.00 (t, J = 5.4 Hz, 1 H, C(b)-H), 3.36 (dd, J = 13.2, 3.9 Hz, 1 H, C(2)-H), 3.31 (m, 2 H, C(a)-H_2), 3.19 (m, 2 H, C(α)-H_2), 3.11 (dd, J = 13.2, 3.9 Hz, 1 H, C(2)-H), 2.71 (s, 3 H, CH_3).

6,8-Bi-S-Cysteinyl-7-[(2-methylamino)ethyl]-3,4-dihydro-5-hydroxy-2H-1,4-Benzothiazine-3-Carboxylic Acid (DHBT-E5)

DHBT-E5 was a very pale pink solid, λ_{max} (pH 2.15) 328 and 260 nm. FAB-MS (glycerol/TFA matrix) gave m/e = 523.1019 (MH^+, 4%, $C_{18}H_{27}N_4O_8S_3$; calcd. m/e = 523.0991). ^1H NMR (D_2O, 50°C) gave δ 6.47 (dd, J = 10.5, 3.9 Hz, 1 H, C(β)-H), 4.94 (t, J = 3.9 Hz, 1 H, C(3)-H), 4.26 (dd, J = 6.9, 4.5 Hz, 1 H, C(b)-H), 4.20 (dd, J = 12.9, 10.5 Hz, 1 H, C(α)-H), 4.18 (dd, J = 6.9, 5.4 Hz, 1 H, C(b′)-H), 3.68 (dd, J = 13.2, 3.9 Hz, 1 H, C(2)-H), 3.61–3.54 (m, 4 H, C(a)-H_2, C(a′)-H_2), 3.51 (dd, J = 13.2, 3.9 Hz, 1 H, C(2)-H), 3.44 (dd, J = 12.9, 3.9 Hz, 1 H, C(α)-H), 3.06 (s, 3 H, CH_3).

6,7-Bi-S-Cysteinyl-8-[(2-methylamino)ethyl]-3,4-dihydro-5-hydroxy-2H-1,4-Benzothiazine-3-Carboxylic Acid (DHBT-E6)

DHBT-E6 was a very pale pink solid that at pH 2.15 exhibited uv bands at λ_{max} 330 (sh), 298 (sh), and 260 nm. FAB-MS (3-nitrobenzyl alcohol matrix) gave m/e = 523.0978 (MH^+, 100%, $C_{18}H_{27}N_4O_8S_3$; calcd. m/e = 523.0991). ^{1}H NMR (D_2O, 50°C) gave δ 6.33 (dd, J = 10.5, 3.9 Hz, 1 H, C(β)-H), 5.03 (t, J = 3.6 Hz, 1 H, C(3)-H), 4.34 (t, J = 5.4 Hz, 1 H, C(b)-H), 4.31 (t, J = 5.4 Hz, 1 H, C(b′)-H), 4.24 (dd, J = 12.9, 10.5 Hz, 1 H, C(α)-H), 3.73 (dd, J = 15.0, 5.4 Hz, 1 H, C(a′)-H), 3.64–3.57 (m, 4 H, C(a′)-H, C(a)-H_2, C(2)-H), 3.45 (dd, J = 12.9, 3.9 Hz, 1 H, C(α)-H), 3.16 (dd, J = 13.2, 3.6 Hz, 1 H, C(2)-H), 3.08 (s, 3 H, CH_3).

5-[(2-Amino-2-carboxyethyl)thio]-6-[(2-methylamino)ethyl]-1,2,3,8,9,10-hexahydrobenzo[1,2-b:4,3-b′]bis[1,4]thiazine-2,9-Dicarboxylic Acid (DHBT-E7)

DHBT-E7 was a pale yellow solid that, when dissolved in the HPLC mobile phase (pH 2.15), exhibited a uv spectrum with a band at λ_{max} 272 nm. FAB-MS (glycerol/TFA matrix) gave m/e = 505.0898 (MH^+, 6%, $C_{18}H_{25}N_4O_7S_3$; calcd. m/e = 505.0885). ^{1}H NMR (D_2O, 60°C) gave δ 6.35 (dd, J = 10.2, 4.5 Hz, 1 H, C(β)-H), 5.08 (t, J = 3.6 Hz, 1 H, C(9′)-H), 4.94 (dd, J = 4.8, 3.3 Hz, 1 H, C(2′)-H), 4.28 (dd, J = 13.2, 10.2, Hz, 1 H, C(α)-H), 4.28 (dd, J = 6.6, 4.8 Hz, 1 H, C(b)-H), 3.67 (dd, J = 13.2, 4.8 Hz, 1 H, C(1′)-H), 3.63 (dd, J = 13.2, 3.6 Hz, 1 H, C(10′)-H), 3.61–3.52 (m, 4 H, C(α)-H, C(a)-H_2, C(1′)-H), 3.29 (dd, J = 13.2, 3.6 Hz, 1 H, C(10′)-H), 3.14 (s, 3 H, CH_3).

RESULTS

Cyclic Voltammetry

A cyclic voltammogram of EPI (0.5 mM) dissolved in phosphate buffer (pH 7.4; μ = 1.0) at a sweep (ν) of 100 mV s^{-1} is presented in Fig. 1A. Peak I_a (peak potential, E_p = 100 mV), observed on the initial anodic sweep, corresponds to the oxidation (2e, 2H^+) of EPI to EPI-*o*-quinone **(1)** that rapidly deprotonates and cylizes to 5,6-dihydroxyindoline **3** (Scheme 1). The latter compound is immediately oxidized by *o*-quinone **1** to give aminochrome **4** (*37*). The reaction sequence EPI → **1** → **2** → **3** → **4** (an eccc mechanism) is so fast that after scan reversal a peak corresponding to the reversible reduction of *o*-quinone **1** cannot be observed in cyclic voltammograms of EPI at pH 7.4 at sweep rates as high as 10 V s^{-1}. Peak II_c (E_p = −255 mV) corresponds to reversible reduction (2e, 2H^+) of aminochrome **4** to **3** and peak II_a (E_p = −248 mV) to the reverse reaction (*37*). Because of the very rapid deprotonation/intramolecular cyclization of **1** to **3** and subsequent oxidation of **3** to **4** by **1**, the peak II_a/peak II_a couple ($E^{\circ\prime}$ = −252 mV) could be observed in cyclic voltammograms of EPI at $\nu \gg 10$ V s^{-1}.

Figure 1B shows a cyclic voltammogram (ν = 100 mV s^{-1}) of EPI (0.5 mM) in the presence of CySH (0.5 mM) at pH 7.4. Under these conditions, the principal effect of CySH is reflected in a significant decrease of the peak current (i_p) for the

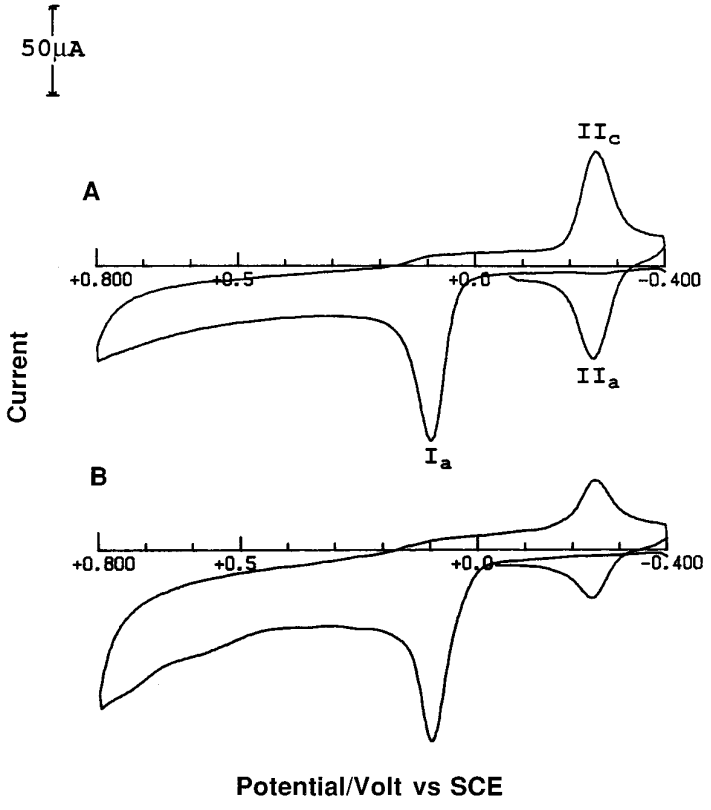

FIG. 1. Cyclic voltammograms at the PGE of 0.5 mM epinephrine (EPI) in pH 7.4 phosphate buffer (μ = 1.0) in the presence of (A) 0 mM CySH and (B) 0.5 mM CySH. Sweep rate: 100 mV s^{-1}.

peak II_c/peak II_a couple. With increasing CySH concentrations (1–5 mM) the peak II_c/peak II_a couple systematically decreases and ultimately disappears (>2.5 mM CySH). Cyclic voltammograms of CySH in pH 7.4 phosphate buffer exhibited no significant oxidation or reduction peaks over the potential range shown in Fig. 1.

Controlled Potential Electro-Oxidation and HPLC Analysis

An HPLC chromatogram of the product solution formed following controlled potential electro-oxidation of EPI (0.5 mM) in the presence of CySH (1.0 mM) in pH 7.4 phosphate buffer at 75 mV for 30 min is presented in Fig. 2. Using preparative HPLC, 11 of the major products of this reaction were isolated and spectroscopically characterized. These included four cysteinyl conjugates of EPI, i.e., 5-*S*-CyS-EPI, 2-*S*-CyS-EPI, 2,5-bi-*S*-CyS-EPI, 2,5,6-tri-*S*-CyS-EPI, 7-[(2-methylamino)ethyl]-3,4-dihydro-5-hydroxy-2*H*-1,4-benzothiazine-3-carboxylic acid (DHBT-E1), and the 6-*S*-cysteinyl-(DHBT-E3) and 6,8-bi-*S*-cysteinyl-(DHBT-E5) conjugates of this DHBT, 8-[(2-methylamino)ethyl]-3,4-dihydro-5-hydroxy-2*H*-1,4-benzothiazine-3-